

Spontaneous formation of concentric waves in a two-component reaction-diffusion system

Takao Ohta,¹ Yumino Hayase,¹ and Ryo Kobayashi²

¹*Department of Physics, Ochanomizu University, Tokyo 112, Japan*

²*Institute for Electronic Science, Hokkaido University, Sapporo 060, Japan*

(Received 17 June 1996)

We carry out computer simulations of an excitable reaction-diffusion equation for an activator and an inhibitor both in one and two dimensions to study various pattern formations such as propagating pulses, and concentric and spiral waves. By choosing a suitable nonlinearity, a stable limit cycle solution can coexist with an equilibrium uniform solution. In this situation, the excitability is still preserved in the sense that a propagating pulse is stable. We have found that propagating pulses do not always annihilate upon collision but cause a domain that emits outgoing wave trains. In two dimensions a concentric wave (target pattern) is formed spontaneously without any pacemaker. The mechanism for these dynamical structures is qualitatively discussed. [S1063-651X(96)03812-3]

PACS number(s): 02.50.-r, 82.20.Mj, 82.30.-b

I. INTRODUCTION

Pattern formation far from equilibrium has attracted much interest recently [1,2]. Experiments of Rayleigh-Benard convection [1–3], the electro hydrodynamic instability of liquid crystals [2,4], chemical reactions [5–8], and crystal growth [9] have put forward our understanding of formation and evolution of patterns significantly. Computer simulations have also disclosed new features of spatiotemporal orders. One of the most intriguing findings is that two pulses (or localized domains) propagating to opposite directions do not always annihilate upon collision as had been believed generally in a dissipative system but exhibit much more complicated dynamical behaviors [10–16].

There are three fundamental properties in a nonvariational nonlinear open system. One is a spatially periodic order. As is well known, this is not realized in a variational system with a short-range interaction. A temporal order such as a limit cycle oscillation is, of course, another characteristic feature far from equilibrium. The third one is an excitability. A steady nonequilibrium state often exhibits a nonlinear response to an external disturbance such that when the disturbance is small, the deviation from the steady state quickly relaxes whereas when the magnitude of the disturbance is beyond certain threshold, the system once goes away from the steady state and then moves back. This kind of nonlinear behavior can never exist in and near thermal equilibrium. An important consequence of the excitability is the existence of a stable propagating pulse and a stable localized domain.

In a theoretical approach to pattern formation, one generally focuses on the slow degrees of freedom. The amplitude equation near a bifurcation point is a typical example [17]. The phase dynamics, which is not necessarily restricted to the vicinity of an instability threshold, is also a powerful method to describe weak deformations around spatially periodic and/or oscillatory order [18]. In fact, the amplitude and the phase dynamics simplify substantially an original model equation of the system and can extract common features of various spatiotemporal patterns.

The amplitude and phase dynamics in their simplest treatment are, however, specific to one bifurcation or a certain

order. Therefore, this theory is not convenient to explore successive bifurcations that are often observed by changing a control parameter in a system. Furthermore, the excitability is not easily incorporated into the theory in terms of the amplitude and the phase.

Another theoretical approach widely employed far from equilibrium is a modeling by a set of reaction-diffusion equations [19]. The above-mentioned three properties can be included simultaneously in a fairly simple reaction-diffusion system. An example is the Bonhoeffer–van der Pol (BvP)–type equation that takes the following form for the variables an activator u and the inhibitor v :

$$\tau \frac{\partial u}{\partial t} = D_u \nabla^2 u + f(u) - v, \quad (1)$$

$$\frac{\partial v}{\partial t} = D_v \nabla^2 v + u, \quad (2)$$

where τ is the ratio of the relaxation rates of u and v . The positive constants D_u and D_v are the diffusion rate of u and v , respectively. $f(u)$ is assumed to have a cubiclike nonlinearity such as

$$f(u) = u(1-u)(u-a) \quad (3)$$

with a a constant.

When D_v is set to be zero, the set of Eqs. (1) and (2) with (3) is known to be excitable. In the opposite limit $D_u \ll D_v$, Eqs. (1) and (2) admit a spatially periodic solution, which is a consequence of a Turing instability [20]. If one replaces $u-a$ by u in (3), the system is oscillatory. Thus, the set of Eqs. (1) and (2) is, despite its simplicity, expected to reveal a variety of bifurcations by changing the parameters. In fact, the BvP-type equation has been applied to various phenomena such as pulse propagation along nerve axons [21], spiral waves in the Belousov-Zhabotinsky reaction [22], biological pattern formation [23,24], and glow discharge [25].

In our previous papers [26–28], we have shown that Eqs. (1) and (2) reveal an essentially new dynamical behavior for a particular choice of $f(u)$:

$$f(u) = \frac{1}{2} \left[\tanh\left(\frac{u-a}{\delta}\right) + \tanh\left(\frac{a}{\delta}\right) \right] - u, \quad (4)$$

where a and δ are positive constants. Note that $f(0)=0$ and the function f becomes piecewise linear in the limit $\delta \rightarrow 0$.

One of the characteristic features of Eqs. (1) and (2) with f given by (4) is that when the diffusion terms are absent, a stable limit cycle coexists with the stable equilibrium solution $u=v=0$ for sufficiently small values of a and δ . In other words, a limit cycle oscillation appears as a subcritical bifurcation by decreasing the parameter a .

A subcritical Hopf bifurcation itself is not special and appears in various nonlinear coupled equations. Near the bifurcation threshold, it is described by the complex Ginzburg-Landau (GL) equation:

$$\frac{\partial W}{\partial t} = d\nabla^2 W + W + p|W|^2 W - q|W|^4 W, \quad (5)$$

where the complex coefficients d, p , and q have positive real parts. We emphasize, however, that Eq. (5) cannot cover the whole properties of Eqs. (1) and (2) in the coexistence region. The excitability still remains in Eqs. (1) and (2) since the oscillation is quite relaxational. In fact, as will be shown in Sec. II, a stable propagating pulse exists in the coexistence region while Eq. (5) does not admit such a solution. This is an essential difference of Eqs. (1) and (2) from Eq. (5) and is the reason why we say that the set of Eqs. (1) and (2) contain the excitability despite the fact that it has a limit cycle oscillation.

Our main concern in the present paper is to investigate what kinds of dynamical order emerge in the system (1) and (2). The parameters D_v and a play the central role of the various types of spatiotemporal structures. Qualitatively, the oscillatory character is strengthened by decreasing the value of a . Since the diffusion of v tends to suppress the growth of the activator u , a propagating pulse becomes unstable for large values of D_v . By further increasing D_v , a localized domain either disappears or becomes motionless depending on the values of a .

The structure of this paper is as follows. An analytical study of Eqs. (1) and (2) is given in Sec. II. We derive the amplitude equation near the Hopf bifurcation and show that the bifurcation is indeed subcritical for small values of the parameter δ in (4). Equations (1) and (2) are solved in the limit $\delta \rightarrow 0$ under the spatially uniform condition. It is shown that a limit cycle solution exists for small values of a . In Sec. III, simulations of a head-on collision of two pulses carry out in one dimension. A localized domain is constituted after the collision, which, in turn, emits pulses propagating outward. We call this oscillatory domain a pulse generator. A pulse generator is also formed starting from a nonuniform initial condition. We investigate the spatiotemporal pattern in detail by changing the parameters a and D_v and obtain a phase diagram of the patterns.

Section IV contains our simulations in two dimensions. A pulse generator in two dimensions causes persistent concen-

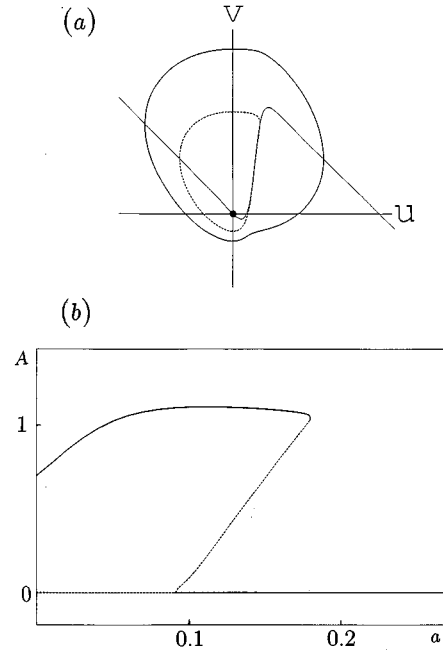


FIG. 1. (a) Limit cycle orbit (thick line) and equilibrium solution (black circle) of Eqs. (1) and (2) for $\delta=0.05$ and $a=0.15$ in the $u-v$ plane. The thin line indicates the function $v=f(u)$ whereas the dotted line means the separatrix. (b) The amplitude of the limit cycle as a function of a . The vertical axis is the maximum value of $(u^2+v^2)^{1/2}$ in one period.

tric waves. The dynamics of spiral waves is also investigated. For example, a two-armed spiral wave can be constructed starting from a suitable initial condition as in an ordinary excitable system. However, a qualitatively different dynamic behavior appears in the core region. That is, the two arms touch each other repeatedly at the core. This is due to the oscillatory character of the system. A brief summary of our results and a discussion of the relationship with other recent simulations are given in Sec. V.

II. LIMIT CYCLE OSCILLATION

In this section, we derive the amplitude equation of Eqs. (1) and (2) near the Hopf bifurcation threshold to obtain the condition where the bifurcation is subcritical for $f(u)$ given by (4). A limit cycle solution is also obtained in the limit $\delta \rightarrow 0$ in (4).

First, we show the numerical results of Eqs. (1) and (2) without the diffusion terms. Figure 1(a) displays the trajectory of the limit cycle in the $u-v$ plane computed for $a=0.15$ and $\delta=0.05$. It is found that when $\delta=0.05$, a limit cycle oscillation exists for $a < a_H = 0.179$. Thus a subcritical Hopf bifurcation occurs at $a = a_H$ by decreasing the value of a . The frequency of oscillation decreases when one decreases the value of a . As far as $f'(0)$ is negative, the equilibrium solution $u=v=0$ is linearly stable. It turns out that $f'(0) > 0$ for $a < a_L = 0.091$. This value is readily obtained from Eq. (4) for $\delta=0.05$. Thus the limit cycle and the equilibrium solution coexist stably for $a_L < a < a_H$. The limit cycle is still stable for $a < a_L$ but the equilibrium solution becomes unstable. The amplitude of oscillation is shown as a function of a in Fig. 1(b).

Next we confirm the subcritical bifurcation obtained above by a reductive perturbation analysis. Since the treatment choosing a as a control parameter is not easy, we here take an alternative approach. Let us write Eqs. (1) and (2) as

$$\frac{\partial u}{\partial t} = D_u \nabla^2 u + f(u) - v, \quad (6)$$

$$\frac{\partial v}{\partial t} = D_v \nabla^2 v + u - \beta, \quad (7)$$

where we have put $\tau=1$ and introduced a constant β in Eq. (7) for convenience. The form of $f(u)$ is not specified but assumed to have three zeros with the smallest one given by $u=0$ and $df/du < 0$ there.

The equilibrium uniform solution u_0 and v_0 is given by

$$u_0 = \beta, \quad (8)$$

$$v_0 = f(\beta). \quad (9)$$

The linear stability of the uniform solution is readily obtained. Put $\vec{s} = (u - u_0, v - v_0) \sim \exp(\lambda t)$. When the deviations \vec{s} are uniform in space, the solution becomes unstable if $f'(\beta)$ is positive where a prime indicates the derivative with respect to the argument. Thus the stability threshold β_c is given through the condition $f'(\beta_c) = 0$, at which the eigenvalue is given by $\lambda = \pm i$.

We introduce the smallness parameter

$$\epsilon^2 = \beta - \beta_c, \quad (10)$$

and expand \vec{s} in powers of ϵ : $\vec{s} = \epsilon \vec{s}_1 + \epsilon^2 \vec{s}_2 + \dots$. At post-threshold, one may put

$$\vec{s}_1 = W(\vec{r}, t) \vec{U} e^{it} + c.c., \quad (11)$$

where c.c. implies complex conjugate. The eigenvector \vec{U} satisfies the relation $L_0 \vec{U} = i \vec{U}$ where the 2×2 matrix L_0 has the elements $L_{00} = L_{22} = 0$ and $L_{12} = -L_{21} = -1$. The complex variable W expresses the slower time dependence of \vec{s}_1 .

By the standard method of reductive perturbation [18], the equation for the amplitude W is calculated up to cubic order as

$$\frac{\partial W}{\partial t} = d \nabla^2 W + \beta_c W - g |W|^2 W, \quad (12)$$

where

$$d = \frac{1}{2} (D_u + D_v), \quad (13)$$

$$g = -\frac{1}{8} f'''(\beta_c) + i \frac{(f'')^2}{12}. \quad (14)$$

If the real part of g is negative, the bifurcation is subcritical. It is readily verified that when $f(u)$ is given by Eq. (4), this indeed occurs for $\delta < \frac{1}{3}$.

In the original set of Eqs. (1) and (2), the constant β is identically zero, which means that the system is below the

threshold. However, since the bifurcation is subcritical, one may expect a stable limit cycle solution as far as the bifurcation point β_c is not much distant from zero. In the nonlinear function (4), this means that the parameter a must be sufficiently small since β_c is close to a . In order to estimate the critical value of a , one needs to evaluate the quartic term in the GL equation. To derive the condition for the existence of a uniform limit cycle solution, we consider the limit $\delta \rightarrow 0$ so that $f(u)$ becomes a piecewise linear form

$$f(u) = -u \quad (15)$$

for $u < a$ and

$$f(u) = -u + 1 \quad (16)$$

for $u > a$.

Here we make a remark. Equations (1) and (2) with $D_v = 0$ and with the piecewise linear dynamics were studied by Rinzel and Keller many years ago [21]. They obtained a propagating pulse solution and a wave train with infinite length and discussed their stability. However, the possibility of a limit cycle solution was not investigated.

Hereafter, for simplicity, we omit the diffusion terms in Eqs. (1) and (2):

$$\frac{du}{dt} = f(u) - v, \quad (17)$$

$$\frac{dv}{dt} = u. \quad (18)$$

An asymptotic periodic solution of Eqs. (17) and (18) can be obtained by the Fourier transform. The variables u and v are expanded as

$$u = \sum_{n=-\infty}^{\infty} C_n \exp\left(\frac{2\pi ni}{T} t\right), \quad (19)$$

$$v = \sum_{n=-\infty}^{\infty} D_n \exp\left(\frac{2\pi ni}{T} t\right), \quad (20)$$

where T is the period of oscillation and is to be determined. Substituting Eqs. (19) and (20) into Eqs. (17) and (18), the Fourier coefficients are readily obtained as

$$C_n = \frac{1 - \exp(-2\pi nit_1/T)}{(2\pi n)^2/T - T - 2\pi ni}, \quad (21)$$

$$D_n = \frac{T}{2\pi ni} C_n, \quad (22)$$

where t_1 is the time interval in one period of oscillation such that u is smaller than a and hence defined through the conditions

$$u(0) = a, u(t_1) = a. \quad (23)$$

The unknown variables T and t_1 can be determined from Eq. (23) as a function of a . Figure 2 shows the result where the full line indicates T whereas the dotted line is t_1 . Note that T and t_1 are multivalued but the lower branch corresponds to

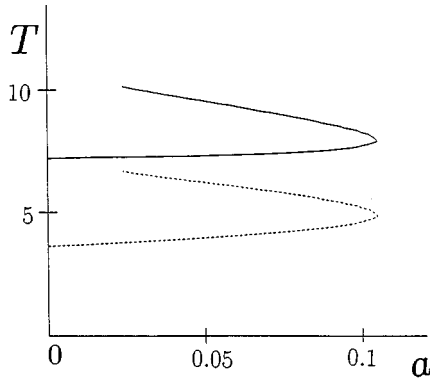


FIG. 2. The period T (full line) and the interval t_1 (dotted line) as a function of a .

the stable limit cycle solution. The period T of a stable limit cycle increases slightly as a is increased. The stable and the unstable limit cycles merge with each other at about $a = 0.107$ and hence beyond this, a limit cycle solution does not exist.

These are consistent with the numerical results shown at the beginning of this section. A slight discrepancy of the threshold value for a is due to the finiteness of the value δ in simulations.

III. PULSE PROPAGATION IN ONE DIMENSION

In Sec. II, we have shown that a stable limit cycle can coexist with a uniform equilibrium state in Eqs. (1) and (2) without the diffusion terms. In this and the next sections, we study the dynamics of Eqs. (1) and (2) when the diffusion is present.

Computer simulations shown below have been carried out for $D_u = 1$, and $\delta = 0.05$ unless stated otherwise and by changing other parameters D_v and a . These parameters alter the dynamical property of the system as follows. Since the amplitude of the limit cycle decreases and the separatrix increases by increasing a as shown in Sec. II, the oscillatory property is weakened for large values of a . As will be shown below, on the other hand, a stable propagating pulse exists for $D_v \rightarrow 0$. It should be noted that this occurs even when a uniform limit cycle solution is also stable. Thus the propagating pulses are expected to have a different property from those in the purely excitable FitzHugh-Nagumo limit of Eqs. (1) and (2) where $D_v = 0$ and $f(u)$ is given, e.g., by Eq. (3). The propagating pulses become less stable if one increases the ratio D_v/D_u . Actually when D_v is sufficiently large, the system undergoes a subcritical Turing instability so that only a motionless pulse or a motionless periodic structure can exist.

It should be noted that the parameter τ is of ordinary magnitude. This is quite in contrast to the previous studies where it is assumed to be extremely small, especially for modeling of the Belousov-Zhabotinsky (BZ) reaction [29]. Smallness of the parameters a and δ in Eq. (4) is also essential in the present problem since the coexistence of the uniform stationary state and a limit cycle oscillation emerges under these conditions.

First, we show numerically that a wave train with arbitrary length is stable for $D_v = 0$ in the coexistence region.

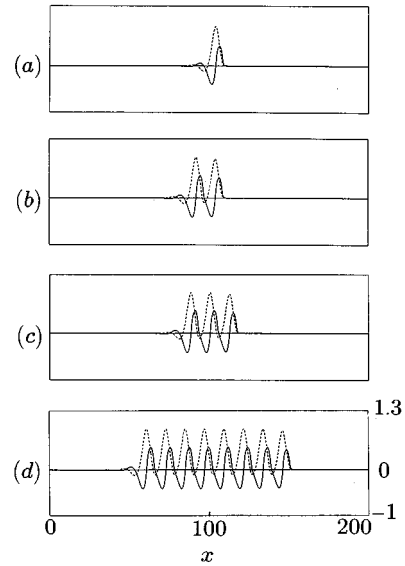


FIG. 3. (a) Pulse and wave trains with the length (b) 2, (c) 3, and (d) 8 for $D_v = 0$ and $a = 0.15$.

Figure 3 displays the wave trains for $a = 0.15$ with various lengths traveling to the right. We have confirmed that the form of these wave trains does not change appreciably in time. For smaller values of a where the oscillatory character is stronger, a wave train with a finite length cannot exist but only an infinitely long wave train appears as a phase wave in an ordinary oscillatory system. When the length of a wave train is finite as in Fig. 3, its propagating velocity is found to be almost independent of the length and is the same as that of a single pulse in Fig. 3(a). This implies that the top train control the velocity.

Now we carry out simulations of a head-on collision of two pulses in one dimension. It is well known that pulses in a dissipative open system generally annihilate upon collision. This is indeed the case in Eqs. (1) and (2) for sufficiently large values of a . We will show, however, that a qualitatively different behavior occurs in the coexistence region. Two single pulses decay upon collision as shown in Fig. 4(a) where $D_v = 0$ and $a = 0.15$. This should be compared with a collision of two-wave trains in Fig. 4(b) for the same values of the parameters. In this process, the front trains annihilate as usual but a localized oscillatory domain forms after the collision of the second trains and furthermore this domain produces sustained pulses propagating outward. We call the localized domain a self-organized pulse generator. It is noted here that the oscillating amplitude of u and v and the period at the center of the domain are almost the same as those of the limit cycle without diffusion.

The formation of a pulse generator can be understood as follows. The initial wave trains act as a trigger wave in the excitable medium. Collision of wave trains produces a large amplitude deviation from the equilibrium solution $u = v = 0$ so that the colliding region enters into the oscillatory state. Thus this phenomenon can be interpreted as a nucleation and growth of the oscillatory state in a uniform state. In fact, one can see from Fig. 4(b) that the region of the pulse generator is gradually expanding with time as if the oscillating domain invades the surrounding quiescent state while emitting the outgoing waves. We have verified for a longer run that the

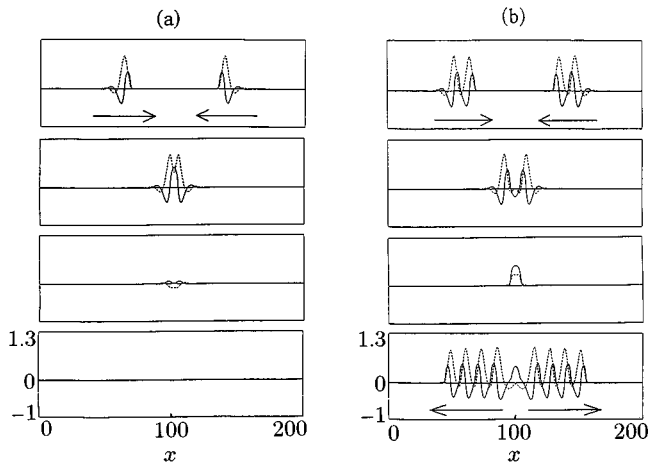


FIG. 4. (a) Collision and annihilation of two single pulses for $D_v=0$ and $a=0.15$. The full (dotted) line indicates the profile of u (v). The time steps are $t=0, 10, 15$, and 20 from top to bottom. (b) Collision of pulse trains and formation of a pulse generator for $D_v=0$ and $a=0.15$. The time steps are $t=0, 20, 30$, and 60 from top to bottom.

speed and the spatial period of the wave train near the oscillating domain gradually increase with time. We believe that this slow change of wave trains is attributed to a phase diffusion since the system is in an oscillatory regime.

It is remarked here that the behavior shown in Fig. 4 is specific to the vicinity of $a=0.15$ where the oscillatory character is not so strong. For smaller values of a , a pulse generator appears even in a collision of two single trains.

A pulse generator can be constructed in an alternative way. That is, a spatially localized domain undergoes spontaneous oscillation and it emits sustained outgoing pulses. We start with the initial condition $u(x,0)=\exp(-x^2/l^2)$ and $v(x,0)=0$ for $-L<x<L$ with the system size $L=100$. Simulations are performed for two different widths $l=1$ and 10 to see the dependence of the initial condition. The Neumann boundary condition is imposed at the system boundaries.

Evolution of the pulse generator and the emitted waves has been studied by changing the parameters D_v and a . Figure 5 summarizes the results for the smaller initial width $l=1$. When D_v is small, typically six different spatiotemporal patterns appear as is indicated, respectively, by I–VI.

Region I is a region where a propagating pulse is stable and the system is strongly oscillatory. An initial localized domain causes a pulse generator that produces stable wave trains as in Fig. 4(b) after collision. Figure 6(a) displays the spatiotemporal pattern observed in region I, where the contour $u=0.001$ is plotted.

In region II where D_v is increased slightly, the initial localized domain still becomes a pulse generator. However, emitted pulse trains do not survive forever. The top train annihilates after a certain lifetime, then the next one disappears, and so forth. Since the speed of a wave train is larger than the decay rate of a front pulse, the front moves slowly outward. Figure 6(b) indicates the behavior for $D_v=0.7$ and $a=0.15$. It is also noted that decay of a pulse does not necessarily occur only at the front of a wave train but also in the middle of a wave train as shown in Fig. 6(c) for $D_v=0.9$. As

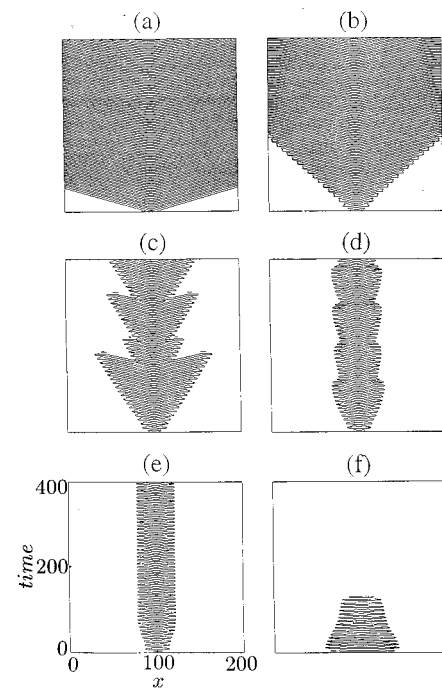


FIG. 5. Phase diagram in D_v - a plane.

mentioned above, the pulse generator is expanding but the velocity of a pulse is almost constant in time so that the distance between two adjacent pulses becomes smaller. When the distance is too small, such a configuration is unstable and one of the pulses disappears. For larger values of

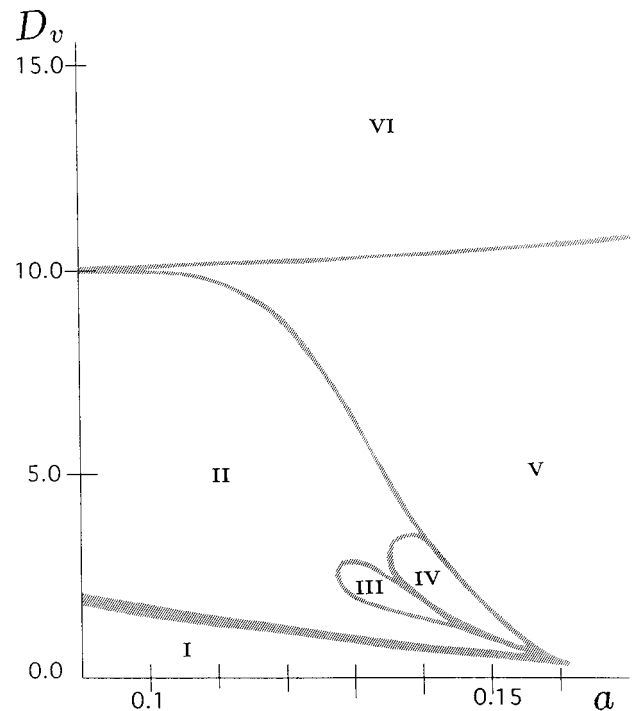


FIG. 6. Spatiotemporal patterns of the pulse generator and the emitted pulses for (a) $D_v=0$, (b) 0.7, (c) 0.9, (d) 1.1, (e) 1.6, and (f) 6.0. The parameter a is fixed as $a=0.15$. The lines indicate the contour lines of $u=0.001$. The abscissa is the space axis whereas the ordinate is the time axis.

D_v where expansion of the pulse generator is negligible, only the front pulse decays.

Some years ago, Ito and Ohta [30] studied analytically the condition for the existence of both motionless and propagating pulses in Eqs. (1) and (2) in the piecewise linear limit $\delta \rightarrow 0$. Comparing with the results obtained there, we note that the boundary between regions I and II shown in Fig. 5 is almost the same (within the numerical uncertainty) as the marginal line in Ref. [30], above which a propagating pulse does not exist. This is clear evidence that the origin of the difference between regions I and II is the stability of a propagating single pulse.

Propagation of the emitted pulses becomes weaker in region III. Figure 6(d) shows an example for $D_v = 1.1$ and $a = 0.15$. It is interesting to see that the size of the oscillating domain is oscillating. This oscillation of the width should not be confused with another type of oscillation of a domain in the BvP equations (1) and (2). It has been reported [31–33] that a stable localized motionless domain, which is a solution of Eqs. (1) and (2) for small values of D_u/D_v , begins to oscillate when one decreases τ . This oscillation, called a breathing motion, originates from the time-delayed interaction between the domain boundaries mediated by the diffusion of v . Therefore, if one puts two localized domains, these undergo an in-phase oscillation. We have examined the interaction of two pulse generators in region III. It seems that the interaction is quite short ranged compared to that of breathing domains.

In the boundary region between regions II and III, complicated spatiotemporal patterns are observed. For instance, the pattern for $D_v = 2.0$ and $a = 0.13$ initially looks like that in Fig. 6(c), but after a long transient it changes to that in Fig. 6(d).

In region IV the localized domain does not emit pulses and the domain width is constant in time. This is because the inhibitor v generated by the reaction in Eq. (1) rapidly diffuses to the surrounding region so that formation of pulses is inhibited. However, the inside of the domain is still oscillating. An example for $D_v = 1.6$ and $a = 0.15$ is shown in Fig. 6(e). By a detailed numerical analysis, we have confirmed that the change from Figs. 6(e) to 6(d) is a supercritical Hopf bifurcation. The domain oscillation in Fig. 6(e) is apparently similar to the breather solution in the nonlinear Schrödinger equation although the present system (1) and (2) is purely dissipative. Probably it is related to the results obtained by Thual and Fauve [34]. They found an oscillation of a localized domain by numerical simulations of the complex GL equation (5) for a subcritical Hopf bifurcation in one and two dimensions. The excitability is nonexistent in region IV since any propagating pulse does not exist there. Thus the system is simply bistable in a sense that a limit cycle and a uniform state coexist. This is the situation expressed by the GL equation.

In region V, the uniform state becomes more stable. When $l = 1$ the domain shrinks and eventually disappears. But if one starts with the larger width $l = 10$, a different pattern is evolved, which will be described shortly below.

When D_v is greater than 10, the initial localized domain does not disappear but tends to form a stable motionless pulse. The boundary between regions V and VI is almost independent of a .

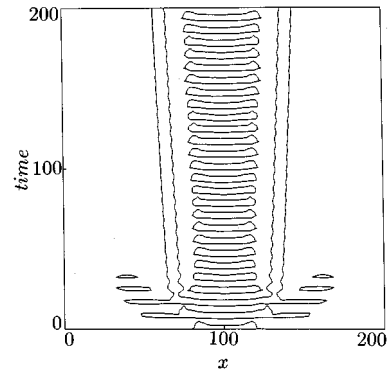


FIG. 7. Spatiotemporal patterns for $D_v = 23$ and $a = 0.11$.

The larger initial width $l = 10$ changes the boundary between regions I and II and other boundaries near $a = 0.17$. The former boundary is not much altered because, as mentioned above, it is the marginal line beyond which a propagating pulse is unstable. Thus, it is intrinsic and insensitive to the initial conditions. Regions II, III, and IV move upward so that the boundary lines between these regions become steeper. For instance, a domain oscillation similar to that in Fig. 6(e) can be observed for $a = 0.14$ and $D_v = 7$. When one starts with the smaller initial width $l = 1$, the domain disappears for these parameters. This fact implies that there is a kind of critical width of the oscillating domain.

A qualitatively different behavior is observed for larger values of D_v . Figure 7 shows the time evolution for $a = 0.11$ and $D_v = 23$ starting with the initial width $l = 10$. In this case, the initial oscillating domain breaks up so that a motionless domain is formed at the tip of the domain while the central part of the original domain is still oscillating. Thus this is a mixed state of regions IV and VI in Fig. 5.

IV. CONCENTRIC AND SPIRAL WAVES

Target pattern and spiral waves have been studied extensively in both excitable and oscillatory systems. In the present system Eqs. (1) and (2), these dynamical behaviors also appear in two dimensions. In this section, we shall show our two-dimensional simulations emphasizing the features different from those of the previous studies.

The persistent outgoing wave train emitted from the pulse generator in one dimension corresponds to a concentric wave (target pattern) in higher dimensions. We have indeed verified numerically that a target pattern emerges from a self-organized pulse generator localized in two dimensions as shown in Fig. 8 where $D_v = 0$ and $a = 0.15$. It is emphasized that the target pattern appears without any heterogeneous pacemaker nor any periodic external stimuli at the center. What is necessary is only an initial concentration deviation.

This property is an essential difference from a target pattern observed in BZ reaction. It is believed that a target pattern in the BZ reaction is caused by some heterogeneity. As mentioned in Sec. III the parameters D_u and τ in Eqs. (1) and (2) with $f(u)$ given by Eq. (3) must be sufficiently small as a model of the BZ reaction [29].

A target pattern can also be constructed from a collision of wave trains in two dimensions as in Fig. 4 in one dimen-

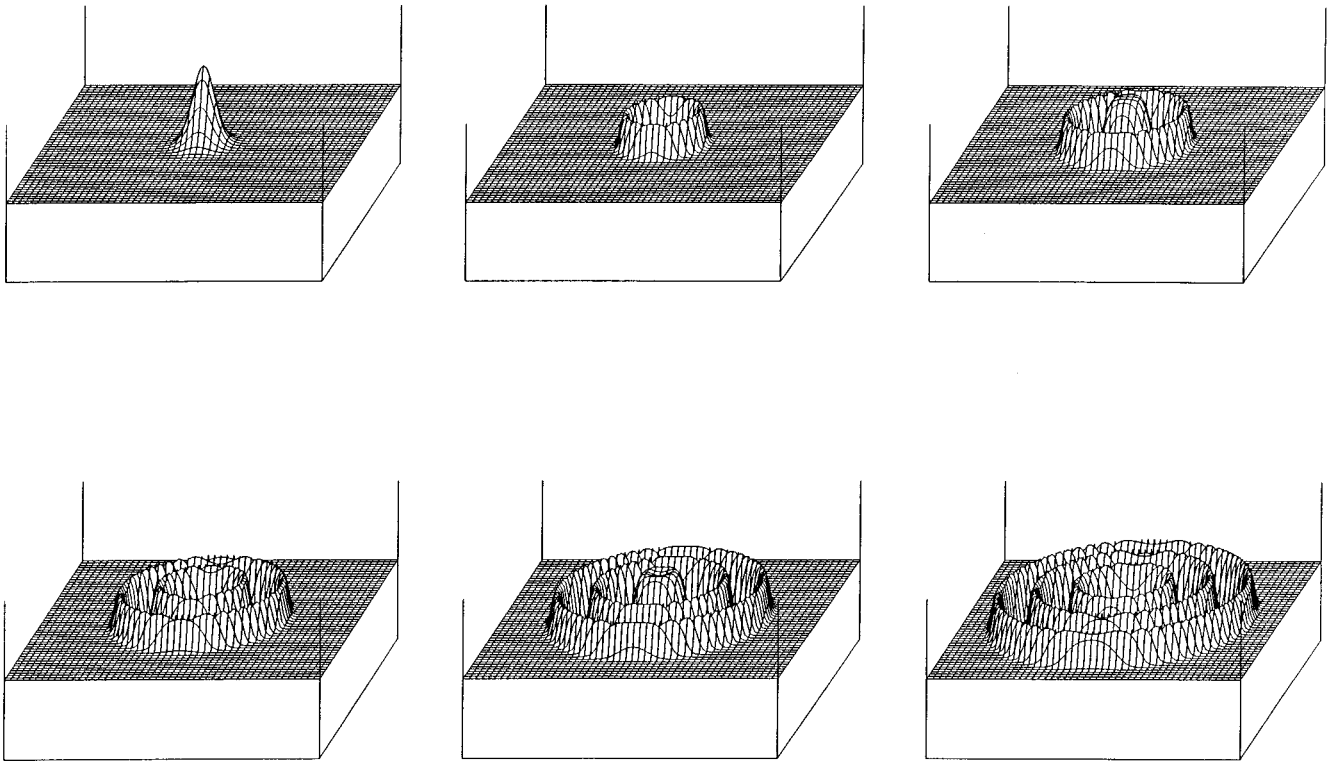


FIG. 8. Time evolution of a target pattern for $D_v=0$ and $a=0.15$. The spatial variation of u is shown at every four time steps from the top left to the bottom right. The system size is 100×100 .

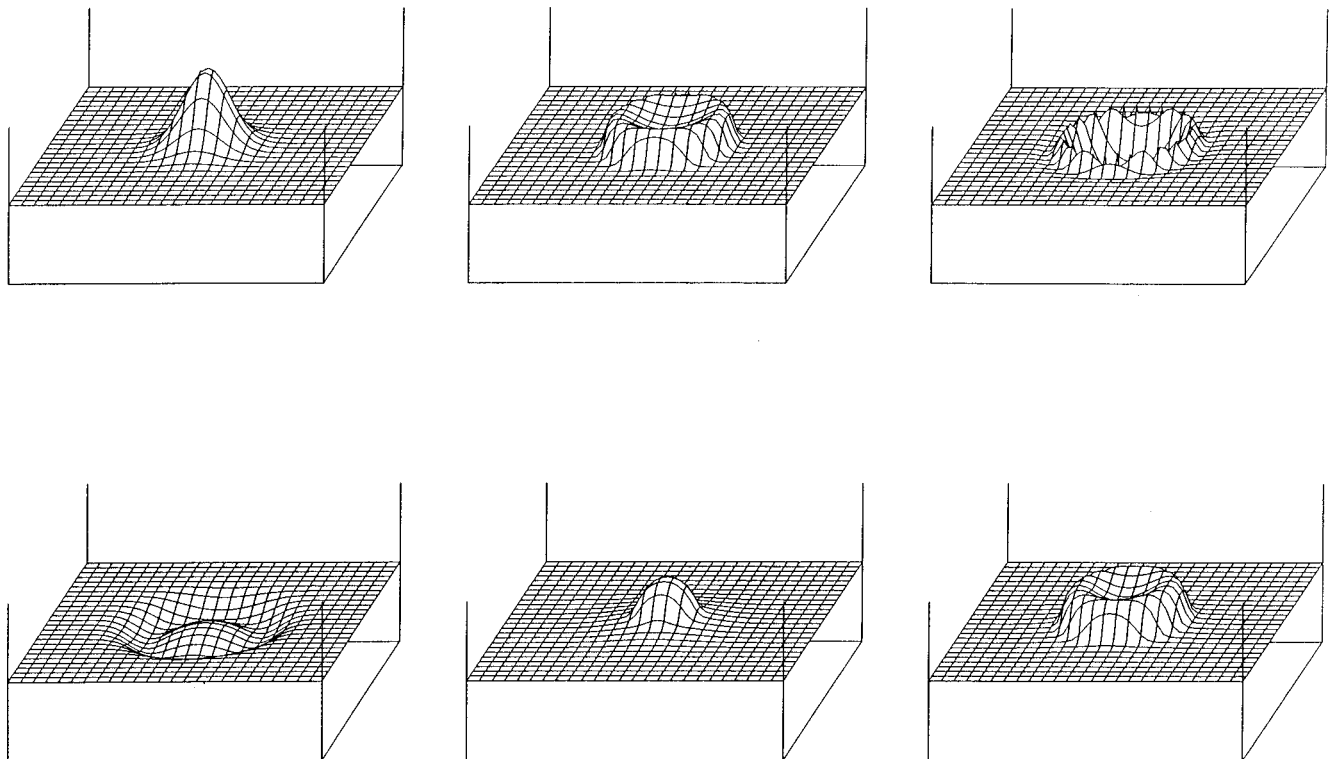


FIG. 9. Oscillating localized domain for $D_u=1$, $D_v=1.2$, and $a=0.15$ at every two time steps. The system size is 50×50 . Other details are the same as those in Fig. 8.

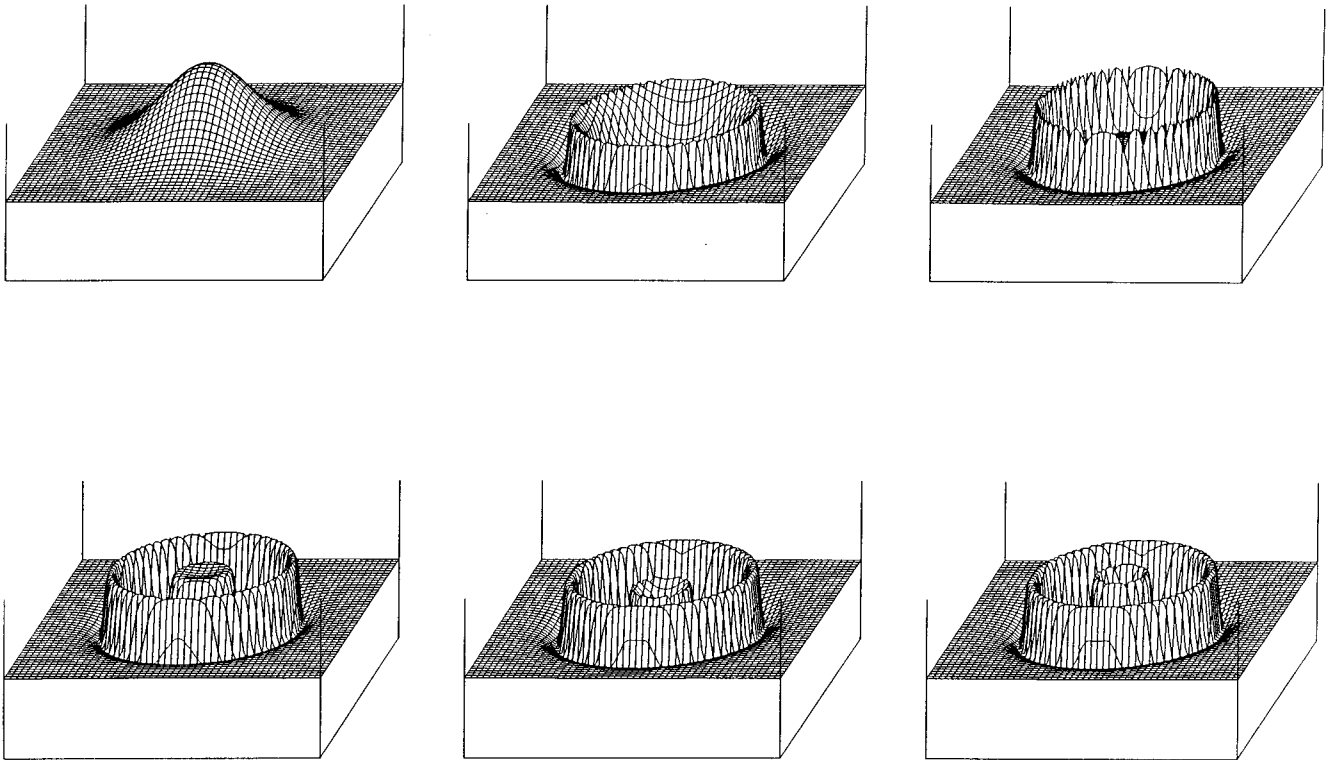


FIG. 10. Formation of a motionless localized target pattern for $D_u=0.25$, $D_v=20.0$, and $a=0.16$ at every four time steps.

sion. A two-dimensional version of a head-on collision is realized by an inward circular wave train. Although not shown in the figure, an inward wave train with one and two rings does not produce a pulse generator but a circular wave train with three rings triggers a pulse generator so that a target pattern is formed. This phenomenon is observed only near $a=0.15$ as in one dimension. Nevertheless, it is remarkable that excitation of outgoing pulses depends on the number of the inward waves, i.e., the number of stimuli.

It is also interesting to see what happens in two dimensions by changing the ratio D_v/D_u . When one increases D_v , the target pattern becomes localized within a certain finite area. Figure 9 depicts a localized target pattern for $D_u=1$, $D_v=1.2$, and $a=0.15$ starting from the initial conditions $u(x,y)=\exp[-(x^2+y^2)/25]$ and $v=0$. This corresponds to Fig. 6(e) in one dimension. When D_u is extremely smaller than D_v , one has an entirely different pattern. In this case, the above initial conditions produce a motionless target pattern as is shown in Fig. 10 for $D_u=0.25$, $D_v=20$, and $a=0.16$.

A spiral wave also exists in the present system. Since it contains both oscillatory and excitable characters, two kinds of spiral waves are possible for the same parameters. One is constructed starting with a planar propagating pulse terminated at one end as in an ordinary excitable system. This is shown in Fig. 11(a). However, if one starts from an initial pulse configuration such that the wavelength of the spiral is short, the system enters into the oscillatory state where the spiral is not a trigger wave but a phase wave. This is evident from the fact that a phase diffusion is observed in this case such that the wavelength increases gradually.

Double-armed or multiarmed spirals can be constructed

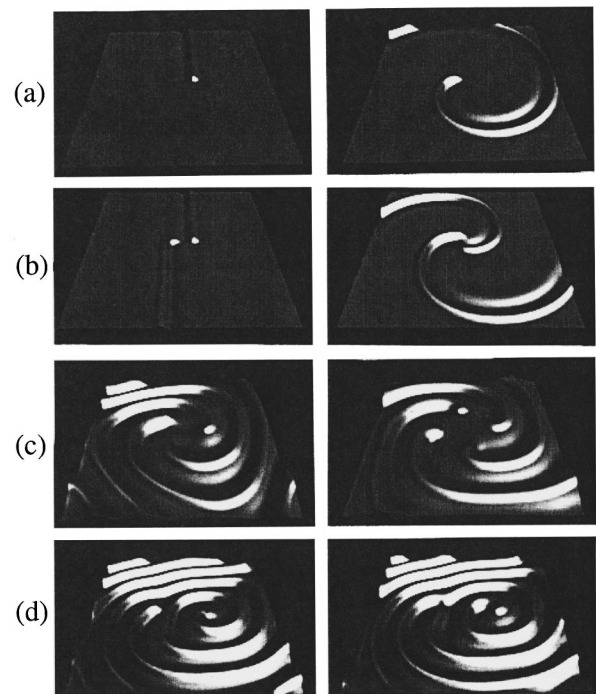


FIG. 11. (a) Formation of a single armed spiral. Time passes from the left to the right. The system size is 100×100 . (b) Formation of a double-armed spiral. (c) Three-armed (left) and four-armed (right) spirals. (d) Defect in a spiral pattern. Note that the location of the defect does not change in time from the left to the right.

for $D_u=1$ and $D_v=0$ in a similar way as shown in Figs. 11(b) and 11(c) for three- and four-armed spirals, respectively. The oscillatory property of the system induces an interesting synchronous motion in the central region. That is, the tips of all the arms stick to and separate from each other periodically. Although the present model is not directly related to the BZ reaction as mentioned above, this motion itself has been observed in the experiments of the BZ reaction [35].

If one starts from an initial condition with lower symmetry, a defect is often formed in a spiral wave as in Fig. 11(d). A wave propagating outward from the core collides with the defect and then a reconnection occurs there. Thus this defect stays at almost the same position and is quite stable.

V. DISCUSSIONS

We have investigated the pattern dynamics of Eqs. (1) and (2) in the parameter regime where a stable limit cycle solution coexists with the uniform equilibrium solution. Propagating pulses are also stable when the diffusion of the inhibitor is small. This implies that the system preserves, to some extent, an excitability. This is one of the most important properties of the system, which is not expressed by a simple complex GL equation for a subcritical Hopf bifurcation.

A pulse generator is self-organized by a collision of pulses or by a local concentration inhomogeneity. In two dimensions, this results in a target pattern both nonlocalized and localized in space depending on the magnitude D_v . The nonlocalized target pattern is different from that observed in the BZ reaction since the latter is believed due to a heterogeneous pacemaker. Actually the frequency of oscillation at the center in the BZ reaction is higher than that in the bulk while, in the present case, it is almost the same as that of a uniform oscillation.

Present simulations show that an extended target pattern can exist in a two-component reaction diffusion system. This is a result that, to our knowledge, has not been seen previously. Computer simulations of a BvP-type model equation for glow discharge [36] have shown automatically excited pulse trains similar to that in Fig. 5(a). However, the time-evolution equation contains a long-range nonlocal interaction. In order to make this interaction short ranged like a

diffusion term, one needs to introduce an extra variable so that the model in Ref. [36] is essentially three variable. Another three-variable model is also proposed for a nonlocalized target pattern [37].

A global phase diagram is obtained in the D_v - a plane. When one increases the value D_v , the target pattern tends to be localized and finally the localized domain becomes either motionless or nonexistent depending on the parameter a and the initial condition.

A target pattern localized in space has been observed experimentally in an electrohydrodynamic instability in liquid crystals [4]. However, this mechanism is interpreted by a coupling of the oscillating mode and a phase of an underlying spatial periodicity [38]. Thus, this localized target pattern is different from that obtained here. As mentioned in Sec. III, a localized oscillatory domain in region IV is closely related to that found numerically in a complex GL equation [34].

At present, only a part of the phase diagram is understood quantitatively. The boundary between regions I and II is given by the stability limit of a single propagating pulse [30]. The motionless domains in the limit $D_u/D_v \ll 1$ are due to a subcritical Turing instability [32,39]. We believe that the essence of the dynamic behaviors in the phase diagram is a nucleation of an oscillatory domain in a quiescent matrix. However, some key factors such as a lifetime of the top pulse in a wave train in region II and a domain size in region IV are not easy to evaluate theoretically. The dependence on the initial conditions as mentioned in Sec. III indicates that there is a critical radius of domain, below which an oscillatory domain does not exist. Our understanding of the critical radius is only semiquantitative [34]. Nevertheless, the present simulations have revealed that the BvP-type Eqs. (1) and (2), which were studied mainly in the singular limit, contain much more fascinating dynamical patterns for the parameters with an ordinary magnitude.

ACKNOWLEDGMENTS

We are grateful to Masayasu Mimura for a number of valuable discussions and comments. Thanks are also due to Daisin Ueyama for his help of visualization of the numerical results. This work was supported by the Grant-in-Aid of Ministry of Education, Science and Culture of Japan.

-
- [1] *Propagation in Systems far from Equilibrium*, edited by J. E. Wesfreid, H. R. Brand, P. Manneville, G. Albinet, and N. Boccara (Springer-Verlag, Berlin, 1988).
 - [2] *Pattern Formation in Complex Dissipative Systems*, edited by S. Kai (World Scientific, Singapore, 1992).
 - [3] P. Manneville, *Dissipative Structures and Weak Turbulence* (Academic, London, 1990).
 - [4] M. Sano, H. Kokubo, B. Jamiaud, and K. Kato, *Prog. Theor. Phys.* **90**, 1 (1993).
 - [5] A. T. Winfree, in *Oscillations and Traveling Waves in Chemical Systems*, edited by R. I. Field and M. Burger (Wiley, New York, 1985).
 - [6] Q. Ouyang and H. L. Swinney, *CHAOS* **1**, 4 (1991).
 - [7] K.-J. Lee, W. D. McCormick, J. E. Pearson, and H. L. Swinney, *Nature (London)* **369**, 215 (1994).
 - [8] K.-J. Lee and H. L. Swinney, *Phys. Rev. E* **51**, 1899 (1995).
 - [9] *Dynamics of Curved Fronts*, edited by P. Pelce (Academic, London, 1988).
 - [10] H. R. Brand and R. J. Deissler, *Phys. Rev. Lett.* **63**, 2801 (1989).
 - [11] R. J. Deissler and H. R. Brand, *Phys. Rev. A* **44**, R411 (1991).
 - [12] H. Sevcikova and M. Marek, in *Bifurcation and Chaos*, edited by R. Seydel *et al.* (Birkhauser Verlag, Basel, 1991).
 - [13] J. E. Pearson, *Science* **261**, 189 (1993).
 - [14] W. N. Reynolds, J. E. Pearson, and S. Ponce-Dawson, *Phys. Rev. Lett.* **72**, 2797 (1994).

- [15] V. Petrov, S. K. Scott, and K. Showalter, *Philos. Trans. R. Soc. London Ser. A* **347**, 631 (1994).
- [16] K. Krisher and A. Mikhailov, *Phys. Rev. Lett.* **73**, 3165 (1994).
- [17] M. Cross and P. C. Hohenberg, *Rev. Mod. Phys.* **65**, 3 (1993).
- [18] Y. Kuramoto, *Chemical Oscillation, Waves and Turbulence* (Springer-Verlag, Berlin, 1984).
- [19] E. Meron, *Phys. Rep.* **218**, 1 (1992).
- [20] A. Turing, *Philos. Trans. R. Soc. London Ser. B* **237**, 32 (1952).
- [21] J. Rinzel and J. B. Keller, *Biophys.* **13**, 1313 (1973).
- [22] J. J. Tyson and J. P. Keener, *Physica D* **32**, 327 (1988).
- [23] H. Meinhardt, *Models of Biological Pattern Formation* (Academic, London, 1982).
- [24] J. D. Murray, *Mathematical Biology* (Springer, Berlin, 1989).
- [25] F.-J. Niedernostheide, R. Dohmen, H. Willebrand, B. S. Kerner, and H.-G. Purwins, *Physica D* **69**, 425 (1993).
- [26] R. Kobayashi, T. Ohta, and Y. Hayase, *Phys. Rev. E* **50**, R3291 (1994).
- [27] T. Ohta, Y. Hayase, and R. Kobayashi, in *Dynamical Systems and Chaos*, edited by Y. Aizawa, S. Saito, and K. Shiraiwa (World Scientific, Singapore, 1995), Vol. 2.
- [28] R. Kobayashi, T. Ohta, and Y. Hayase, *Physica D* **84**, 162 (1995).
- [29] J. J. Tyson and P. C. Fife, *J. Chem. Phys.* **73**, 2224 (1980).
- [30] A. Ito and T. Ohta, *Phys. Rev. A* **45**, 8374 (1992).
- [31] S. Koga and Y. Kuramoto, *Prog. Theor. Phys.* **63**, 106 (1980).
- [32] B. Kerner and V. V. Osipov, *Usp. Fiz. Nauk* **157**, 201 (1989) [*Sov. Phys. Usp.* **32**, 101 (1989)].
- [33] T. Ohta, M. Mimura, and R. Kobayashi, *Physica D* **34**, 115 (1989).
- [34] O. Thual and S. Fauve, *J. Phys. (Paris)* **49**, 182 (1988).
- [35] T. Yamaguchi (unpublished).
- [36] C. Radehaus, R. Dohmen, H. Willebrand, and F.-J. Niedernostheide, *Phys. Rev. A* **42**, 7426 (1990).
- [37] A. S. Mikhailov, *Physica D* **55**, 99 (1992).
- [38] H. Sakaguchi, *Prog. Theor. Phys.* **87**, 1049 (1992).
- [39] T. Ohta, A. Ito, and A. Tetsuka, *Phys. Rev. A* **42**, 3225 (1990).